

SPECIAL SOLUTIONS TO A COMPACT EQUATION FOR DEEP-WATER GRAVITY WAVES

FRANCESCO FEDELE* AND DENYS DUTYKH

ABSTRACT. Recently, Dyachenko & Zakharov (2011) [9] have derived a compact form of the well known Zakharov integro-differential equation for the third order Hamiltonian dynamics of a potential flow of an incompressible, infinitely deep fluid with a free surface. In this work, special traveling wave solutions of this compact equation are numerically constructed using the Petviashvili method. Their stability properties are also investigated. Further, unstable traveling waves with wedge-type singularities, viz. peakons, are numerically identified. An analytical solution of such peakons is derived also for a perturbed version of the compact equation. Finally, by means of an accurate Fourier-type spectral scheme it is found that smooth solitary waves appear to collide elastically, suggesting the integrability of the Zakharov equation.

CONTENTS

1. Introduction	1
2. Envelope dynamics and special solutions	3
2.1. A Hamiltonian Dysthe equation	4
2.2. Ground states and traveling waves	6
3. Traveling wave interactions	8
3.1. Numerical method description	8
3.2. Numerical results	10
4. Conclusions	12
Acknowledgements	13
References	13

1. INTRODUCTION

The Euler equations that describe the irrotational flow of an ideal incompressible fluid of infinite depth with a free surface are Hamiltonian. Their symplectic formulation was discovered by [36] in terms of the free-surface elevation $\eta(x, t)$ and the velocity potential $\varphi(x, t) = \phi(x, z = \eta(x, t), t)$ evaluated at the free surface of the fluid. Here, $\eta(x, t)$ and $\varphi(x, t)$ are conjugated canonical variables with respect to the Hamiltonian \mathcal{H} given by the total wave energy. It is well known that the Euler equations are completely integrable

Key words and phrases. water waves; deep water approximation; Hamiltonian structure; travelling waves; solitons.

* Corresponding author.

in several important limiting cases. For example, in a two-dimensional (2-D) ideal fluid, unidirectional weakly nonlinear narrowband wave trains are governed by the Nonlinear Schrödinger (NLS) equation, which is integrable [40]. Integrability also holds for certain equations that models long waves in shallow waters, in particular the Korteweg–de Vries (KdV) equation (see, for example, [1, 2, 6, 34]) or the Camassa–Holm (CH) equation [4]. For these equations, the associated Lax-pairs have been discovered and the Inverse Scattering Transform [1, 2, 6, 34] unveiled the dynamics of solitons, which elastically interact under the invariance of an infinite number of time-conserving quantities.

Another important limiting case of the Euler equations for the free-surface of an ideal flow is that considered by Zakharov [36, 37]. By means of a third order expansion of \mathcal{H} in the wave steepness, he derived an integro-differential equation in terms of canonical conjugate Fourier amplitudes, which has no restrictions on the spectral bandwidth. To derive the Zakharov (Z) equation, fast non-resonant interactions are eliminated via a canonical transformation that preserves the Hamiltonian structure [17, 37]. The integrability of the Z equation is still an open question, but the fully nonlinear Euler equations are non-integrable [7, 8]. Indeed, non-integrability can be easily proven by considering the terms of the perturbation series of the Hamiltonian in powers of the wave steepness limited on their resonant manifolds. To have non integrability, it is enough to prove that at least one of these amplitudes is nonzero. In this regard, Dyachenko & Zakharov [7, 8] conjectured that the Z equation for unidirectional water waves (2-D) is integrable since the nonlinear fourth-order term of the Hamiltonian vanishes on the resonant manifold, leaving only trivial wave-wave interactions, which just cause nonlinear frequency shifts of the separate Fourier modes. They also pushed their analysis to the next order and proved that the effective fifth-order term does not vanish on the corresponding resonant manifold. Thus, the Euler equations of the free-surface hydrodynamics are not integrable in two dimensions and also in three-dimensional (3-D) flows [8].

Recently, Dyachenko and Zakharov (2011) [9] realized that the trivial resonant quartet-interactions that occur in the 2-D free surface dynamics could be further removed by a canonical transformation. As a result, the Z equation drastically simplifies to the compact form

$$ib_t = \Omega b + \frac{i}{8} \left(b^* (b_x^2)_x - (b_x^* (b^2)_x)_x \right) - \frac{1}{4} \left[b \mathbf{K} \{ |b_x|^2 \} - (b_x \mathbf{K} \{ |b|^2 \})_x \right], \quad (1.1)$$

where b is the new canonical variable and b_t, b_x denote partial derivatives with respect to t and x and the symbols of the pseudo-differential operators Ω and \mathbf{K} are given, respectively, by $\sqrt{g|k|}$ and $|k|$, where k is the Fourier transform parameter. Further, b scales with the wave surface η as $b \sim \sqrt{\frac{2g}{\omega_0}} \eta$.

In this study, we explore (1.1), hereafter referred to as cDZ, for analytical studies and numerical investigations of special solutions in the form of solitary waves. The present paper is organized as follows. First, we derive the envelope equation associated to cDZ and then ground states and traveling waves are numerically computed using the Petviashvili method ([26], see also [18]). Particular solutions with wedge-type singularities, viz. peakons, are also numerically identified. Analytical solutions of such singular structures

are derived for a perturbed version of the local form of cDZ equation (1.1), where the non-local terms involving the operator \mathbf{K} are neglected. Finally, the interaction of traveling waves is numerically investigated by means of an accurate Fourier-type pseudo-spectral scheme.

2. ENVELOPE DYNAMICS AND SPECIAL SOLUTIONS

Consider the following ansatz for wave trains in deep water

$$b(X, T) = \varepsilon \sqrt{\frac{2g}{\omega_0}} a_0 B(X, T) e^{i(X-T)}, \quad (2.1)$$

where B is the envelope of the carrier wave $e^{i(X-T)}$, and $X = \varepsilon k_0(x - c_g t)$, $T = \varepsilon^2 \omega_0 t$, with $k_0 = \frac{\omega_0}{g}$ and ω_0 as characteristic wavenumber and frequencies. The small parameter $\varepsilon = k_0 a_0$ is a characteristic wave steepness and c_g is the wave group velocity in deep water. The envelope B associated to the wave surface η is then expressed as

$$\eta(X, T) = \varepsilon a_0 B(X, T) e^{i(X-T)} + \text{c.c.}, \quad (2.2)$$

where *c.c.* denotes complex conjugation. Using (2.1) in (1.1) yields the cDZ envelope equation

$$\begin{aligned} iB_T &= \Omega_\varepsilon B + \frac{i}{4} (B^* \mathcal{S}((SB)^2) + iB^*(SB)^2 - 2\mathcal{S}(B|SB|^2)) \\ &\quad - \frac{\varepsilon}{2} [B\mathbf{K}\{|SB|^2\} - \mathcal{S}(SB\mathbf{K}\{|B|^2\})], \end{aligned} \quad (2.3)$$

where $\mathcal{S} = \varepsilon \partial_X + i$. The approximate dispersion operator Ω_ε is defined as follows

$$\Omega_\varepsilon := \frac{1}{8} \partial_{XX} + \frac{i}{16} \varepsilon \partial_{XXX} - \frac{5}{128} \varepsilon^2 \partial_{XXXX} + \frac{7i}{256} \varepsilon^3 \partial_{XXXXX},$$

where $o(\varepsilon^3)$ dispersion terms are neglected. Equation (2.3) admits three invariants, viz. the action \mathcal{A} , momentum \mathcal{M} and the Hamiltonian \mathcal{H} given, respectively, by

$$\mathcal{H} = \int_{\mathbb{R}} \left[B^* \Omega_\varepsilon B + \frac{i}{4} |SB|^2 [B(SB)^* - B^* SB] - \frac{\varepsilon}{2} |SB|^2 \mathbf{K}(|B|^2) \right] dx, \quad (2.4)$$

$$\mathcal{A} = \int_{\mathbb{R}} B^* B dx, \quad \mathcal{M} = \int_{\mathbb{R}} i(B^* SB - B(SB)^*) dx. \quad (2.5)$$

Expanding the operator \mathcal{S} in terms of ε , (2.3) can be written in the form of a generalized derivative NLS equation as

$$iB_T = \Omega_\varepsilon B + |B|^2 B - 3i\varepsilon |B|^2 B_X - \frac{\varepsilon}{2} B\mathbf{K}\{|B|^2\} + \varepsilon^2 \mathcal{N}_2(B) + \varepsilon^3 \mathcal{N}_3(B) = 0, \quad (2.6)$$

where

$$\begin{aligned} \mathcal{N}_2(B) &= -\frac{3}{2} B^* (B_X)^2 + B |B_X|^2 - |B|^2 B_{XX} + \frac{1}{2} B^2 B_{XX}^* + \\ &\quad \frac{i}{2} [B\mathbf{K}(B^* B_X - B B_X^*) + B_X \mathbf{K}|B|^2 + (B\mathbf{K}|B|^2)_X], \end{aligned}$$

and

$$\mathcal{N}_3(B) = -\frac{i}{2}|B_X|^2 B_X + \frac{i}{2}B_{XX}(B^* B_X - BB_X^*) - \frac{1}{2}BB_X B_{XX}^* - \frac{1}{2}\left[B\mathbf{K}|B_X|^2 - (B_X\mathbf{K}|B|^2)_X\right].$$

To leading order the NLS equation is recovered.

2.1. A Hamiltonian Dysthe equation. Hereafter, we will study a special case of (2.6), which is a symplectic version of the temporal Dysthe equation [11]. Keeping terms to $O(\varepsilon)$ in (2.6) yields

$$iB_T = \left(\frac{1}{8}\partial_{XX} + \frac{i\varepsilon}{16}\partial_{XXX}\right)B + |B|^2 B - 3i\varepsilon|B|^2 B_X - \frac{1}{2}\varepsilon B\mathbf{K}|B|^2, \quad (2.7)$$

hereafter referred to as cDZ-Dysthe. The original temporal Dysthe equation written in terms of B (see (2.1)) is given by

$$iB_T = \left(\frac{1}{8}\partial_{XX} + \frac{i\varepsilon}{16}\partial_{XXX}\right)B + i|B|^2 B - 3\varepsilon i|B|B_X - \varepsilon i\beta B^2 B_X^* + \varepsilon B\mathbf{K}(|B|^2) = 0,$$

where $\beta = 1/4$. This equation is not Hamiltonian since expressed in terms of multiscale variables, which are usually non canonical (see, for example, [12]). Indeed, it differs from (2.7) by the term $\beta B^2 B_X^*$. As noted by Hogan (1985) [16] such term does not play any role in the linear stability of uniform wave trains within the order of truncation of the perturbation analysis leading to the Dysthe equation. However, in three dimensions the β term yields a better confinement of the instability region for the Stokes wave and the associated Dysthe equations are less susceptible to numerical instability and energy leakage [31]. Recently, another canonical form (which does not contain the β term) has been derived by Gramstad & Trulsen (2011) [15] starting from the Hamiltonian Z equation with the Krasitskii kernel [17], viz.

$$iB_T = \left(\frac{1}{8}\partial_{XX} + \frac{i\varepsilon}{16}\partial_{XXX}\right)B + |B|^2 B - 3i\varepsilon|B|^2 B_X - \varepsilon B\mathbf{K}|B|^2.$$

This equation has the same structure as the cDZ-Dysthe (2.7), however the coefficients of the non-local terms are different. This may be so because the cDZ-Dysthe is a special case of the compact form of the Z equation. We also point out that Zakharov & Dyachenko (2010) [38], starting from a conformal-mapping formulation of the Euler equations derived another version of the temporal Dysthe equation, which is similar to (2.7) but also non-Hamiltonian.

The original Dysthe model as other mathematical models used in physics and mechanics do not always possess a canonical Hamiltonian structure. Typically, the dynamics is governed by partial differential equations expressed in terms of physically-based variables, which are not usually canonical. A transformation to new variables is needed in order to unveil the desired structure explicitly (see, for example, [27]). This is the case for the equations of motion for an ideal fluid: in the Eulerian description, they cannot be recast in a canonical form, whereas in a Lagrangian frame the Hamiltonian structure is revealed by Clebsch potentials (see, for example, [27, 24]). Moreover, multiple-scale perturbations of differential equations expressed in terms of non-canonical variables typically lead to approximate equations that do not maintain the fundamental conserved quantities, as the

hydrostatic primitive equations on the sphere [22], where energy and angular momentum conservation are lost under the hydrostatic approximation.

As an example, consider the finite dimensional system of an harmonic oscillator in the classical canonical variables $q(t)$ (coordinate) and $p(t)$ (momentum). This admits the canonical form

$$\dot{q} = \frac{\partial \mathcal{H}}{\partial p} = p, \quad \dot{p} = -\frac{\partial \mathcal{H}}{\partial q} = -q, \quad (2.8)$$

where \dot{p} denotes time derivative, and $\mathcal{H} = (q^2 + p^2)/2$. The flow in the phase-space is 'incompressible' since the divergence vanishes:

$$\frac{\partial \dot{q}}{\partial q} + \frac{\partial \dot{p}}{\partial p} = 0.$$

The transformation $z = q + ip$ is canonical and (2.8) transforms to

$$\dot{z} = -i \frac{\partial \mathcal{H}}{\partial z^*} = -iz, \quad \dot{z}^* = i \frac{\partial \mathcal{H}}{\partial z} = iz^*, \quad (2.9)$$

where $\mathcal{H} = |z|^2/2$, and z^* is the complex conjugate of z . It is straightforward to prove that the gauge transformation

$$z = we^{i\alpha|w|^2},$$

with α as a free parameter, is also canonical, and (2.9) remains unchanged in the new variables w and w^* . On the other hand, if one considers the coordinate change

$$Q = \frac{q}{\sqrt{1 + \alpha q^2}}, \quad P = p, \quad (2.10)$$

then (2.8) transforms to the noncanonical form

$$\dot{P} = -Q \left(\sqrt{1 + \alpha P^2} - 2\alpha P^2 \right), \quad \dot{Q} = \frac{P}{\sqrt{1 + \alpha P^2}}. \quad (2.11)$$

This flow does not preserve volume as (2.8) does, nonetheless equations (2.11) are those of a disguised harmonic oscillator obtained via the noncanonical change of variables (2.10) (see also [24]). The original Dysthe equation [11] shares the same roots as (2.11). They both come from a noncanonical transformation of a Hamiltonian system. For the spatial version of the Dysthe equation, canonical variables have been identified by means of a gauge transformation, and the hidden Hamiltonian structure is unveiled [12]. The more general transformation proposed by Dyachenko & Zakharov (2011) [9] yields the symplectic form (2.7) of the original temporal Dysthe equation [11].

In the following, insights into the underlying dynamics of cDZ equation and associated Dysthe are to be gained if we construct some special families of solutions in the form of ground states and traveling waves, often just called solitons or solitary waves, as described below.

2.2. Ground states and traveling waves. To begin, consider the cDZ equation (2.3). We construct numerically ground states and traveling waves (TW) of the form $B(X, T) = F(X - cT)e^{-i\omega T}$, where c and ω are generic parameters and the function $F(\cdot)$ is in general complex. After substituting this ansatz into the governing equation (2.3) we obtain the following nonlinear steady problem (in the moving frame $X - cT$)

$$\mathcal{L}F = \mathcal{N}(F),$$

where $\mathcal{L} = \omega - ic - \Omega_\varepsilon$ and $\mathcal{N}(F)$ denotes nonlinear terms of the cDZ of (2.3). In order to solve this equation we use the Petviashvili method [26, 25, 18, 35]. This numerical approach has been successfully applied in deriving TWs of the spatial version of the Dysthe equation [12]. Schematically, the iteration takes the following form

$$F_{n+1} = \mathcal{S}^\gamma \mathcal{L}^{-1} \cdot \mathcal{N}(F_n), \quad \mathcal{S} = \frac{\langle F_n, \mathcal{L} \cdot F_n \rangle}{\langle F_n, \mathcal{N}(F_n) \rangle},$$

where \mathcal{S} is the so-called stabilizing factor and the exponent γ is usually defined as a function of the degree of nonlinearity p ($p = 3$ for the cDZ equation). The rule of thumb prescribes the following formula $\gamma = \frac{p}{p-1}$. The scalar product is defined in the L_2 space. The inverse operator \mathcal{L}^{-1} can be efficiently computed in the Fourier space. To initialize the iterative process, one can use the analytical solution to the leading order NLS equation (see the associated Dysthe equation (2.7)). We point out that this method can be very efficiently implemented using the Fast Fourier Transform (FFT) (see, for example, [13]).

Without losing generality, hereafter we just consider the leading term of the dispersion operator, viz. $\Omega_\varepsilon = \frac{1}{8}\partial_{xx}$, since the soliton shape is only marginally sensitive to the higher order dispersion terms as shown in Figure 1. Figure 2 shows the action \mathcal{A} of the ground states ($c = 0$, but moving with the group velocity in the physical frame) as a function of the frequency ω computed via the Petviashvili iteration and numerical continuation for $\varepsilon = 0.20$. The stability of a ground state is investigated numerically by means of an accurate Fourier-type spectral scheme [3, 30], see also [12]. We found that smooth ground states are stable in agreement with the criterion formulated by Vakhitov & Kolokolov (1973) [32], since $\frac{d\mathcal{A}}{d\omega} > 0$ (see also [39, 35]). Further, we notice that an abrupt reduction in the action \mathcal{A} occurs at a critical frequency $\omega_c(\varepsilon)$ and solitons with wedge-type singularities, viz. peakons, bifurcate from a smooth solitary waves as shown in the right panel of Figure 2. Clearly, this bifurcation can be interpreted as a possible indication of the non-existence of smooth solitons above the critical threshold ω_c . As one can see, as ω increases the soliton shape tends to become asymmetric and steeper until the critical threshold $\omega_c = 0.85$, above which the smooth solitary waves bifurcate to peakons, which are unstable in agreement with [32], since $\frac{d\mathcal{A}}{d\omega} < 0$. Peakons also bifurcate from smooth solitons of given frequency ω as the steepness ε increases, as clearly seen in Figure 3. Note that in both cases ground states grow asymmetrically before bifurcating to smaller peakons, and so do travelling waves ($c \neq 0$). However, such bifurcation is not observed in the 2-D NLS or Dysthe equations (see, for example, [12]), as clearly seen in Figures 5 – 7 where we report the dependence of the three invariants \mathcal{A} , \mathcal{M} and \mathcal{H} on the parameters ω , c and ε for the cDZ and cDZ-Dysthe equations respectively.

We point out that stable and elastic peakons have been discovered in a special limit of the integrable CH equation [4]. On the contrary, from numerical investigations of the cDZ equation peakons appear unstable. The left panel of Figure 4 shows the numerically converged peakon obtained via the Petviashvili scheme using $N \sim 1.5 \times 10^6$ Fourier modes for $\varepsilon = 0.20$. A slight Gibbs phenomenon is observed in the numerical solution of peakons due to the derivative discontinuity at the peak, even though we have used a large number of Fourier modes in the Petviashvili scheme.

As the frequency ω increases, peakons bifurcate at smaller steepness ε as clearly seen in the right panel of Figure 4. Indeed, for ground states we observed numerically that $\omega_c(\varepsilon) \sim \varepsilon^{-2}$ (see left panel of Figure 8), and the same scaling holds also for travelling waves ($c \neq 0$). In the physical frame (x, t) , owing to the scaling $T = \varepsilon^2 \omega_0 t$, bifurcation occurs at a well defined frequency $\omega = \varepsilon^2 \omega_c \approx 0.037 \omega_0$, which is independent of ε . Further, in the domain X both the peakon amplitude $a_p = |B|_{X=0^-}$ and the associated slope of the wedge singularity (corner)

$$s_p = \frac{1}{a_p} \partial_X |B|_{X=0^-} = \cot(\theta/2)$$

scales as $\varepsilon^{-3/2}$, θ being the interior angle of the peakon's singularity (see central and right panels of Figure 7). In the physical frame x , from (2.2) the slope s_p becomes

$$s_p = \varepsilon a_0 \partial_X |B|_{X=0^-} \partial_x X = \varepsilon^3 a_p s_p \approx \cot(170^\circ/2),$$

which is independent of ε and corresponds to an angle $\theta \approx 170^\circ$. Note that Longuet-Higgins and Fox [20, 21, 19] in their asymptotic theory for the almost-highest solitary wave found that $\theta \approx 120^\circ$. Thus the numerical peakon is flatter than their ultimate solitary wave. Such difference may be attributed to the fact that their theory accounts for nonlinearities of all orders, whereas the cDZ equation considers third order nonlinear effects in terms of canonical variables. These numerical results on the existence of peakons are corroborated by an analytical solution of such singular structures for a perturbed version of the local cDZ, viz.

$$iB_T = \Omega_\varepsilon B + \frac{i}{4} (B^* \mathcal{S}((\mathcal{S}B)^2) + (1 + \delta) i B^* (\mathcal{S}B)^2 - 2\mathcal{S}(B|\mathcal{S}B|^2)), \quad (2.12)$$

where δ is a real parameter (for $\delta = 0$ the local form of cDZ is recovered). Analytical peakons in the form of traveling waves are given by

$$B(X, T) = a e^{i(\kappa X - \omega_p T)} e^{-\alpha^2 |X - c_p T|}, \quad (2.13)$$

where a is an arbitrary parameter and

$$\kappa = -\frac{8 + \delta}{8\varepsilon}, \quad \alpha^2 = \frac{|\delta|}{8\varepsilon}, \quad \omega_p = -\frac{4 + \delta}{32\varepsilon^2}, \quad c_p = \frac{8 + \delta}{32\varepsilon}.$$

Clearly, for $\delta = 0$ the peakon reduces to a periodic wave solution of the local cDZ. Thus, peakons can bifurcate from periodic waves of the local cDZ as δ changes sign. Note also that ground states occur for $\delta = -8$. Figure 9 shows an example of a numerical peakon ($\delta = 1$ and $\varepsilon = 0.3$) computed using the Petviashvili scheme (Fourier modes $N \sim 1.5 \times 10^6$) and the corresponding analytical solution (2.13). The agreement between the numerical

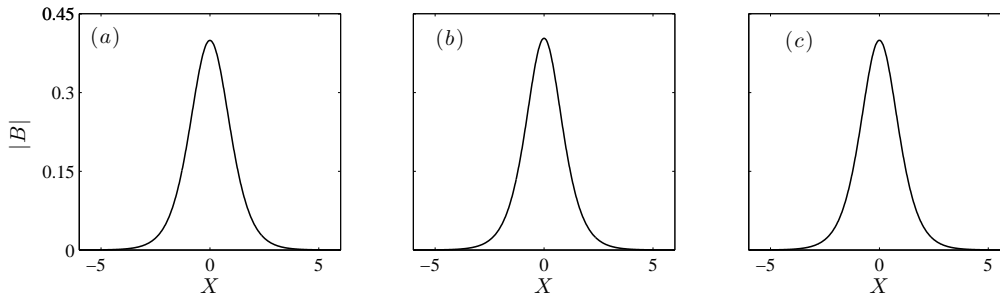


FIGURE 1. cDZ equation: Convergence of the solution with respect to the dispersion relation approximation: the second, third and fifth orders (from left to right). We have to indicate also the numerical parameters.

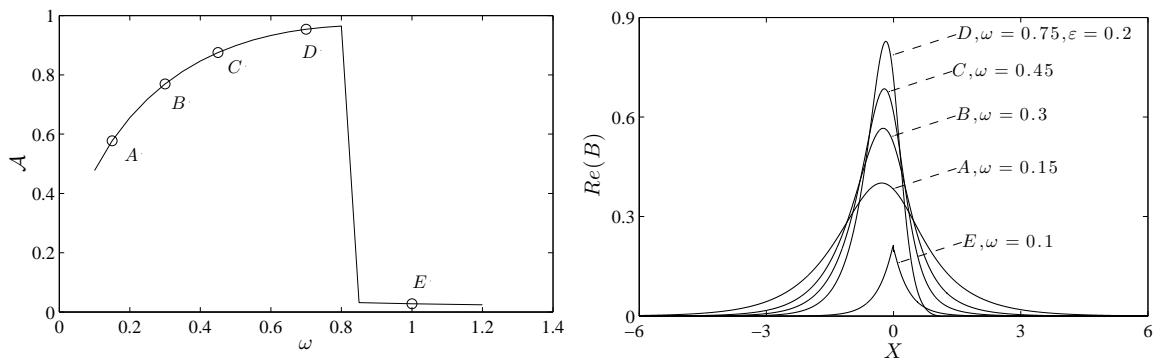


FIGURE 2. cDZ equation: (left) Action \mathcal{A} of ground states as function of the frequency ω and (right) bifurcation of a peakon from smooth ground states ($\varepsilon = 0.2$).

and analytical solutions is remarkable. Finally, note that the analytical peakon (2.13) has a slope that scales as ε^{-1} , in contrast to the $\varepsilon^{-3/2}$ scaling observed numerically for the full cDZ singular solution. In the physical frame x , the associated interior angle of the wedge singularity is independent of ε and just function of δ , and so is the peakon frequency ω_p in agreement with the numerical cDZ peakons. This is an indirect evidence of the validity of our numerical results for the cDZ equation.

3. TRAVELING WAVE INTERACTIONS

Hereafter, we investigate the collision of smooth traveling waves of the cDZ equation (2.3) by means of a highly accurate Fourier-type pseudo-spectral method. We will first briefly describe the adopted spectral approach and then discuss the numerical results.

3.1. Numerical method description. We rewrite (2.3) in the operator form

$$B_t + \mathcal{L} \cdot B = \mathcal{N}(B), \quad (3.1)$$

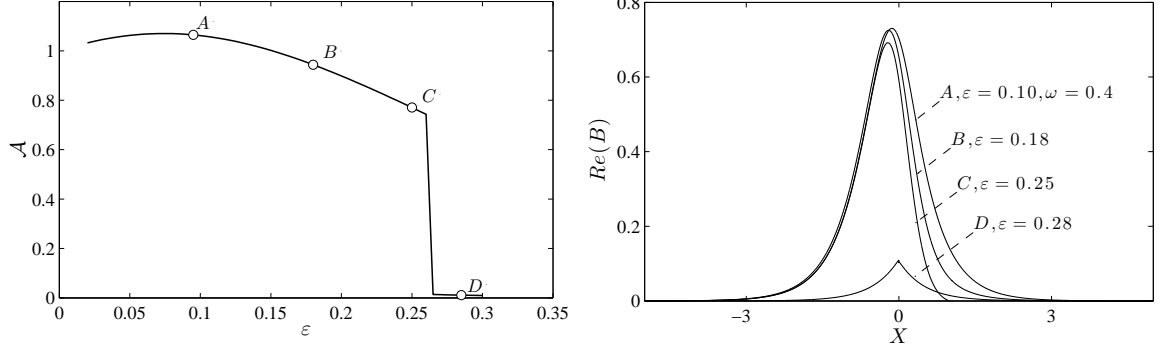


FIGURE 3. cDZ equation: (left) Action \mathcal{A} of ground states as function of the steepness ε and (right) bifurcation of a peakon from smooth ground states ($\omega = 0.4$).

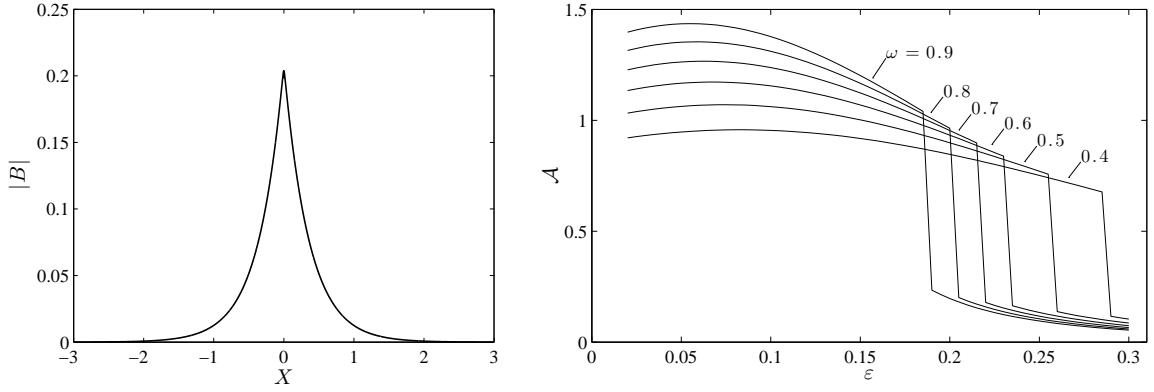


FIGURE 4. cDZ peakon: (left) numerical solution via the Petviashvili scheme ($\varepsilon = 0.2$, number of Fourier modes $N \sim 1.5 \times 10^6$) and (right) action of ground states as function of the steepness epsilon for different values of the frequency ω .

where $\mathcal{L} = i\frac{1}{8}\partial_{XX}$ and

$$\mathcal{N}(B) = \frac{1}{4}(B^*\mathcal{S}((\mathcal{S}B)^2) + iB^*(\mathcal{S}B)^2 - 2\mathcal{S}(B|\mathcal{S}B|^2)) + \frac{\varepsilon i}{2}[\mathbf{BK}\{|SB|^2\} - \mathcal{S}(\mathcal{S}B\mathbf{K}\{|B|^2\})].$$

We solve (3.1) numerically by applying the Fourier transform in the space variable X . The transformed functions will be denoted by $\hat{B} = \mathcal{F}\{B\}$. We recall that the symbol of the non-local term is equal to $|k|$, and that of \mathcal{L} is $i\frac{1}{8}k^2$, k being the Fourier transform parameter. The nonlinear terms are computed in physical space, while space derivatives ∂_X and the Hilbert transform \mathbf{K} are computed in Fourier space. For example, the term B^2B_X is discretized as

$$\mathcal{F}\{B^2B_X\} = \mathcal{F}\{(\mathcal{F}^{-1}(\hat{B}))^2 \cdot \mathcal{F}^{-1}\{ik\hat{B}\}\},$$

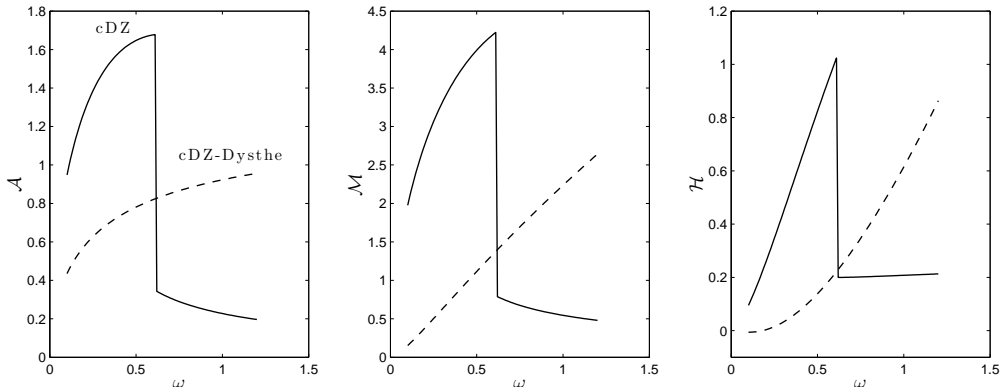


FIGURE 5. cDZ equation: Action \mathcal{A} , momentum \mathcal{M} and Hamiltonian \mathcal{H} dependence on the frequency ω for travelling waves ($\varepsilon = 0.23$, $c = 0$).

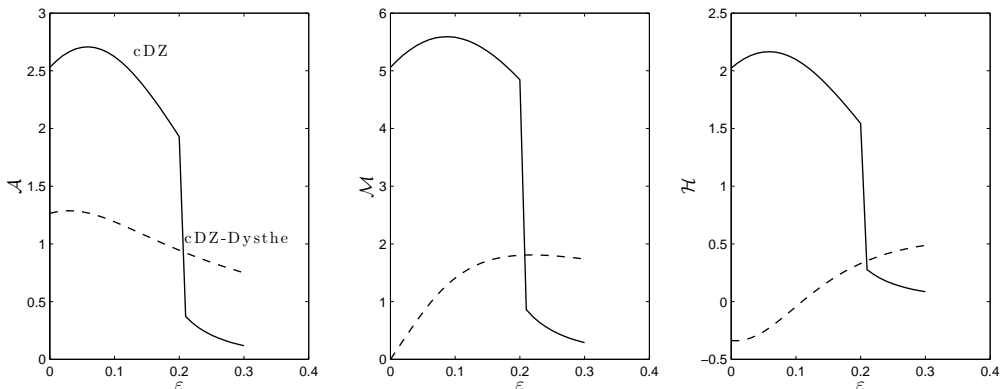


FIGURE 6. cDZ equation: Action \mathcal{A} , momentum \mathcal{M} and Hamiltonian \mathcal{H} dependence on the steepness parameter ε for travelling waves ($\omega = 0.80$, $c = 0$).

and all nonlinear terms are treated in a similar way. We note that the usual 4/3 rule is applied for anti-aliasing since we have to deal with cubic nonlinearities [30, 5, 14].

In order to improve the stability of the space discretization procedure, we can integrate exactly the linear terms. This is achieved by making a change of variables [23, 14]:

$$\hat{W}_t = e^{(t-t_0)\mathcal{L}} \cdot \mathcal{N} \left\{ e^{-(t-t_0)\mathcal{L}} \cdot \hat{W} \right\}, \quad \hat{W}(t) \equiv e^{(t-t_0)\mathcal{L}} \cdot \hat{B}(t), \quad \hat{W}(t_0) = \hat{B}(t_0).$$

Finally, the resulting system of ODEs is discretized in space by the Verner's embedded adaptive 9(8) Runge–Kutta scheme [33]. The step size is chosen adaptively using the so-called H211b digital filter [28, 29] to meet the prescribed error tolerance, set as of the order of machine precision.

3.2. Numerical results. In all the performed simulations the accuracy has been checked by following the evolution of invariants (2.4), (2.5). From a numerical point of view the

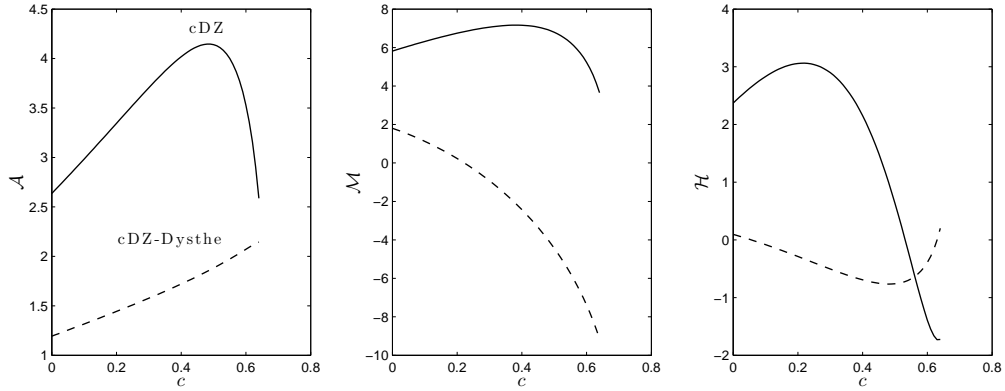


FIGURE 7. cDZ equation: Action \mathcal{A} , momentum \mathcal{M} and Hamiltonian \mathcal{H} dependence on the velocity c for travelling waves ($\varepsilon = 0.12$, $\omega = 0.90$).

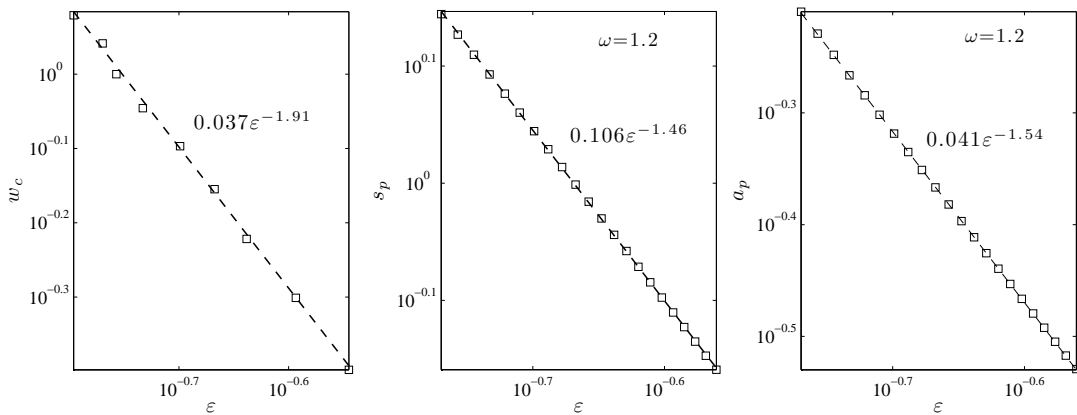


FIGURE 8. cDZ peakon: Dependence of the critical frequency ω_c , peakon slope s_p and amplitude a_p on the steepness parameter ε . This result is obtained for ground states. However, the same scalings hold true also for the travelling waves as well.

cDZ equation becomes gradually stiffer as the steepness parameter ε increases, or if higher order dispersion terms are included. Consequently, the conservation of invariants \mathcal{H} , \mathcal{A} and \mathcal{M} might be degraded. Nevertheless, even in the stiffest situations a decent accuracy was assured by choosing a sufficiently large number of Fourier modes and the dispersion operator $\Omega_\varepsilon = \frac{1}{8}\partial_{xx}$. For example, for $\varepsilon = 0.10$ the number $N = 16384$ of Fourier modes were sufficient to achieve conservation of the invariants close to $\sim 10^{-13}$. As an application, consider the interaction between two solitary waves traveling in opposing directions with the same speed ($\varepsilon = 0.10$). The plot of Figure 10 shows that the two solitons emerge out of the collision with the same shape, but a slight phase shift. The interaction appears elastic as clearly seen from the plot of Figure 11, which reports the initial and final shapes of the two solitary waves. Further, the interaction of two traveling waves with a ground

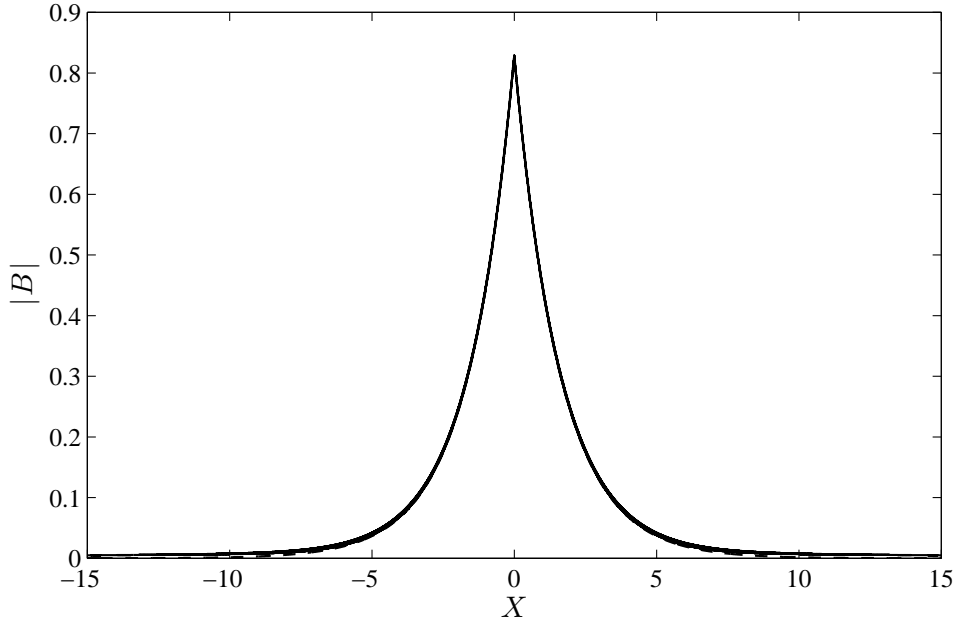


FIGURE 9. Numerical peakon (solid) of the perturbed local cDZ equation (2.12) and associated analytical solution (2.13) (dash) for $\varepsilon = 0.30$.

state appears also elastic (see Figures 12 – 13). This suggests the integrability of the cDZ equation (2.3) in agreement with the recent results of Dyachenko *et al.* (2012) [10]. However, the associated Hamiltonian version of the Dysthe equation (2.7) does not support elastic collisions as shown in Figure 14.

4. CONCLUSIONS

Special solutions of the compact Zakharov equation in the form of traveling waves are numerically constructed using the Petviashvili method. The stability of ground states agrees with the Vakhitov-Kolokolov criterion. Further, unstable ground states with wedge-type singularities, viz. peakons, are numerically identified bifurcating from smooth ground states. In the physical frame (x, t) , the interior angle θ of the peakon's discontinuity is $\approx 170^\circ$. Thus, the numerical peakon is flatter than the almost-highest solitary wave proposed by Longuet-Higgins and Fox [20, 21, 19]. Similar conclusions also hold for the traveling waves of the cDZ. Further, an analytical peakon in the form of a traveling wave solution is found for a perturbed version of the local form of the cDZ equation. Moreover, such peakons are unstable, in contrast to the stable and elastic ones of the CH equation. Finally, by means of an accurate Fourier-type pseudo-spectral scheme, it is also shown that smooth solitary waves appear to collide elastically, suggesting the integrability of the compact Zakharov equation, but not that of the associated Hamiltonian version of the Dysthe equation.

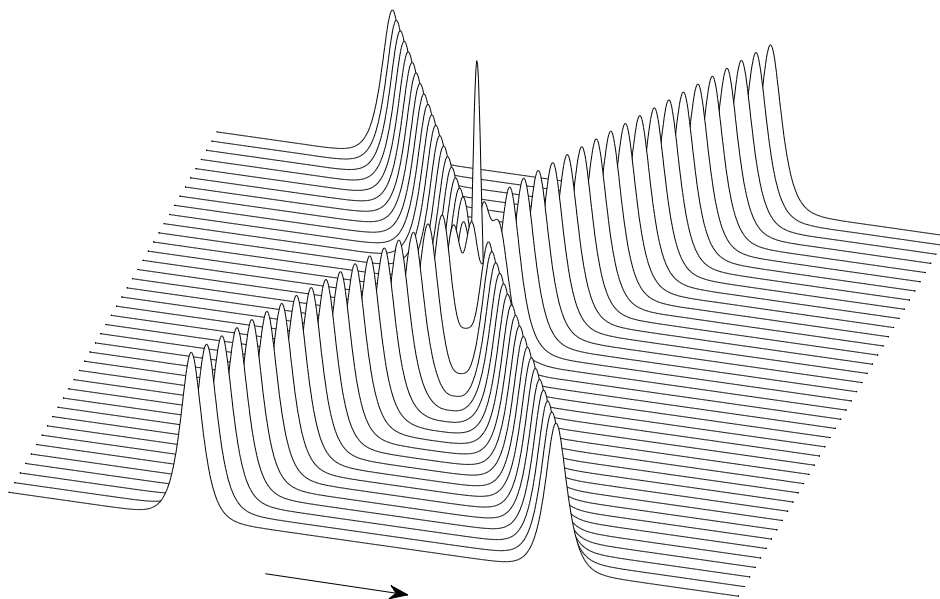


FIGURE 10. cDZ Equation: collision of two smooth travelling waves ($\varepsilon = 0.10$).

ACKNOWLEDGEMENTS

D. Dutykh acknowledges the support from French Agence Nationale de la Recherche, project MathOcéan (Grant ANR-08-BLAN-0301-01).

REFERENCES

- [1] M. J. Ablowitz, D. J. Kaup, A. C. Newell, and H. Segur. The inverse scattering transform-Fourier analysis for nonlinear problems. *Stud. Appl. Math.*, 53:249–315, 1974. [2](#)
- [2] M. J. Ablowitz and H. Segur. *Solitons and the Inverse Scattering Transform*. Society for Industrial & Applied Mathematics, 1981. [2](#)
- [3] J. P. Boyd. *Chebyshev and Fourier Spectral Methods*. 2nd edition, 2000. [6](#)
- [4] R. Camassa and D. Holm. An integrable shallow water equation with peaked solitons. *Phys. Rev. Lett.*, 71(11):1661–1664, 1993. [2](#), [7](#)
- [5] D. Clamond and J. Grue. A fast method for fully nonlinear water-wave computations. *J. Fluid. Mech.*, 447:337–355, 2001. [10](#)
- [6] P. G. Drazin and R. S. Johnson. *Solitons: An introduction*. Cambridge University Press, Cambridge, 1989. [2](#)

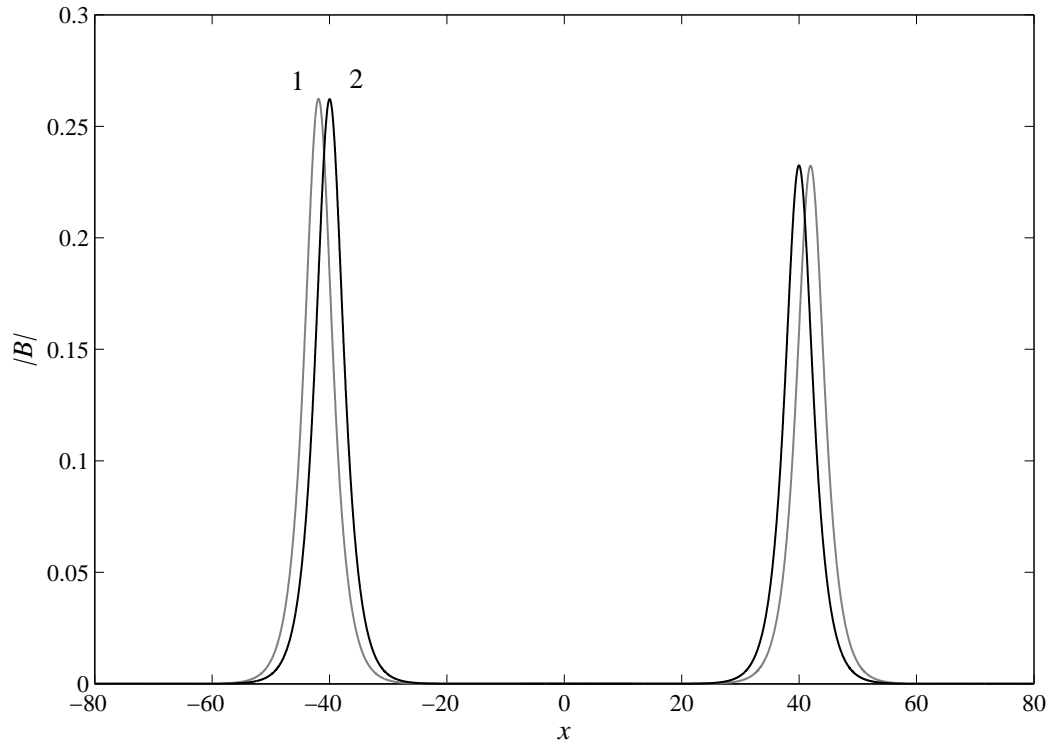


FIGURE 11. cDZ equation: Initial (1) shape and (2) after collision of the two interacting traveling waves of Figure 10.

- [7] A. I. Dyachenko and V. Zakharov. Is free-surface hydrodynamics an integrable system? *Physics Letters A*, 190(2):144–148, 1994. [2](#)
- [8] A. I. Dyachenko and V. Zakharov. Toward an integrable model of deep water. *Physics Letters A*, 221(1-2):80–84, 1996. [2](#)
- [9] A. I. Dyachenko and V. E. Zakharov. Compact Equation for Gravity Waves on Deep Water. *JETP Lett.*, 93(12):701–705, 2011. [1](#), [2](#), [5](#)
- [10] A. I. Dyachenko, V. E. Zakharov, and D. I. Kachulin. Collision of two breathers at surface of deep water. *Arxiv:1201.4808*, page 15, 2012. [12](#)
- [11] K. B. Dysthe. Note on a modification to the nonlinear Schrödinger equation for application to deep water. *Proc. R. Soc. Lond. A*, 369:105–114, 1979. [4](#), [5](#)
- [12] F. Fedele and D. Dutykh. Hamiltonian form and solitary waves of the spatial Dysthe equations. *JETP Lett.*, 94(12):921–925, October 2011. [4](#), [5](#), [6](#)
- [13] M. Frigo and S. G. Johnson. The Design and Implementation of FFTW3. *Proceedings of the IEEE*, 93(2):216–231, 2005. [6](#)
- [14] D. Fructus, D. Clamond, O. Kristiansen, and J. Grue. An efficient model for three-dimensional surface wave simulations. Part I: Free space problems. *J. Comput. Phys.*, 205:665–685, 2005. [10](#)
- [15] O. Gramstad and K. Trulsen. Hamiltonian form of the modified nonlinear Schrödinger equation for gravity waves on arbitrary depth. *J. Fluid Mech.*, 670:404–426, 2011. [4](#)
- [16] S. J. Hogan. The 4th-order evolution equation for deep-water gravity-capillary waves. *Proc. R. Soc. A*, 402(1823):359–372, 1985. [4](#)

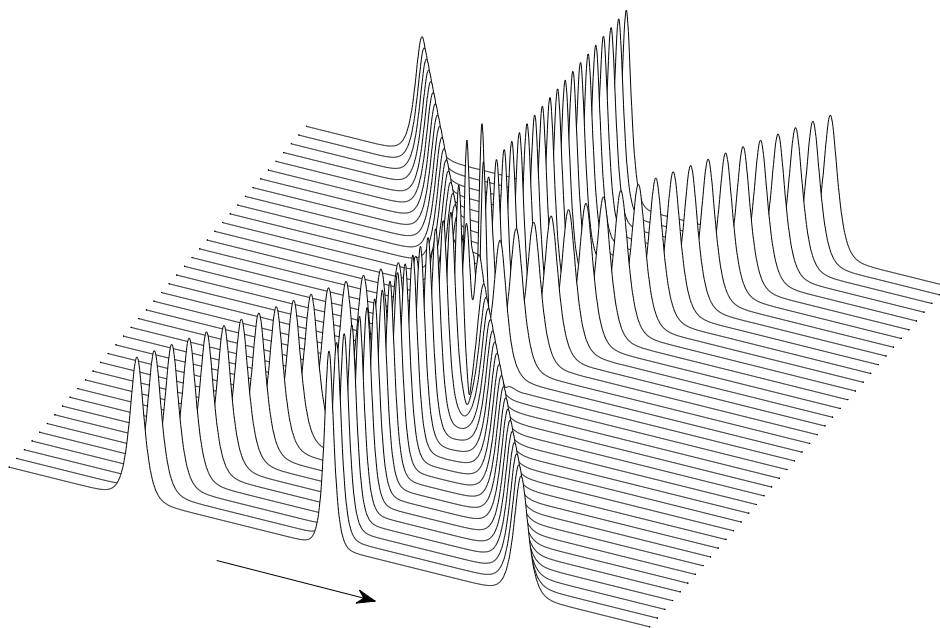


FIGURE 12. cDZ equation: Elastic collision of two traveling waves with a ground state ($\varepsilon = 0.10$).

- [17] V. P. Krasitskii. On reduced equations in the Hamiltonian theory of weakly nonlinear surface waves. *J. Fluid Mech.*, 272:1–20, 1994. [2](#), [4](#)
- [18] T. I. Lakoba and J. Yang. A generalized Petviashvili iteration method for scalar and vector Hamiltonian equations with arbitrary form of nonlinearity. *J. Comp. Phys.*, 226:1668–1692, 2007. [2](#), [6](#)
- [19] M. S. Longuet-Higgins and J. H. Fox. Asymptotic theory for the almost-highest solitary wave. *J. Fluid Mech.*, 317:1–19, 1996. [7](#), [12](#)
- [20] M. S. Longuet-Higgins and M. J. H. Fox. Theory of the almost-highest wave: the inner solution. *J. Fluid Mech.*, 80:721–741, April 1977. [7](#), [12](#)
- [21] M. S. Longuet-Higgins and M. J. H. Fox. Theory of the almost-highest wave. Part 2. Matching and analytic extension. *Journal of Fluid Mechanics*, 85:769–786, April 1978. [7](#), [12](#)
- [22] E. N. Lorenz. Energy and numerical weather prediction. *Tellus*, 12:364–373, 1960. [5](#)
- [23] P. Milewski and E. Tabak. A pseudospectral procedure for the solution of nonlinear wave equations with examples from free-surface flows. *SIAM J. Sci. Comput.*, 21(3):1102–1114, 1999. [10](#)
- [24] P. J. Morrison. Hamiltonian description of the ideal fluid. *Rev. Mod. Phys.*, 70(2):467–521, 1998. [4](#), [5](#)

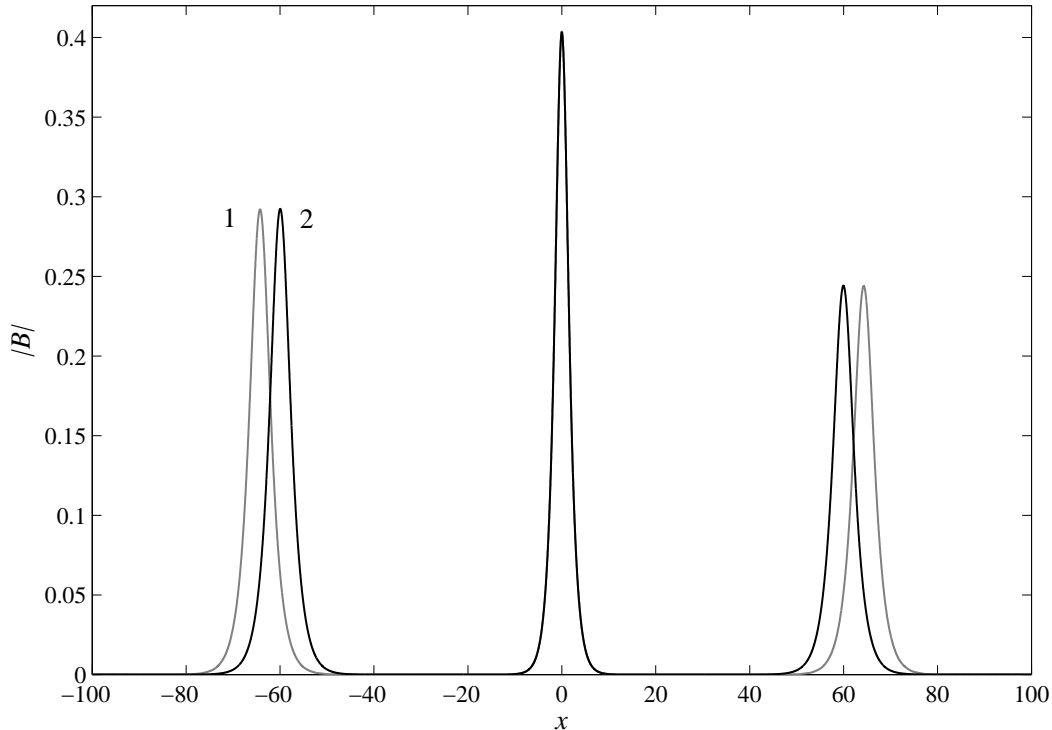


FIGURE 13. cDZ equation: Initial (1) shape and (2) after collision of the three solitons of Figure 12.

- [25] D. Pelinovsky and Y. A. Stepanyants. Convergence of Petviashvili's iteration method for numerical approximation of stationary solutions of nonlinear wave equations. *SIAM J. Num. Anal.*, 42:1110–1127, 2004. [6](#)
- [26] V. I. Petviashvili. Equation of an extraordinary soliton. *Sov. J. Plasma Phys.*, 2(3):469–472, 1976. [2](#), [6](#)
- [27] R. L. Seliger and G. B. Whitham. Variational principle in continuous mechanics. *Proc. R. Soc. Lond. A*, 305:1–25, 1968. [4](#)
- [28] G. Söderlind. Digital filters in adaptive time-stepping. *ACM Trans. Math. Software*, 29:1–26, 2003. [10](#)
- [29] G. Söderlind and L. Wang. Adaptive time-stepping and computational stability. *Journal of Computational and Applied Mathematics*, 185(2):225–243, 2006. [10](#)
- [30] L. N. Trefethen. *Spectral methods in MatLab*. Society for Industrial and Applied Mathematics, Philadelphia, PA, USA, 2000. [6](#), [10](#)
- [31] K. Trulsen and K. B. Dysthe. Frequency downshift in three-dimensional wave trains in a deep basin. *J. Fluid Mech.*, 352:359–373, 1997. [4](#)
- [32] N. G. Vakhitov and A. A. Kolokolov. Stationary solutions of the wave equation in a medium with nonlinearity saturation. *Radiophysics and Quantum Electronics*, 16(7):783–789, July 1973. [6](#)
- [33] J. H. Verner. Explicit Runge-Kutta methods with estimates of the local truncation error. *SIAM J. Num. Anal.*, 15(4):772–790, 1978. [10](#)
- [34] G. B. Whitham. *Linear and nonlinear waves*. John Wiley & Sons Inc., New York, 1999. [2](#)
- [35] J. Yang. *Nonlinear Waves in Integrable and Nonintegrable Systems*. SIAM, 2010. [6](#)

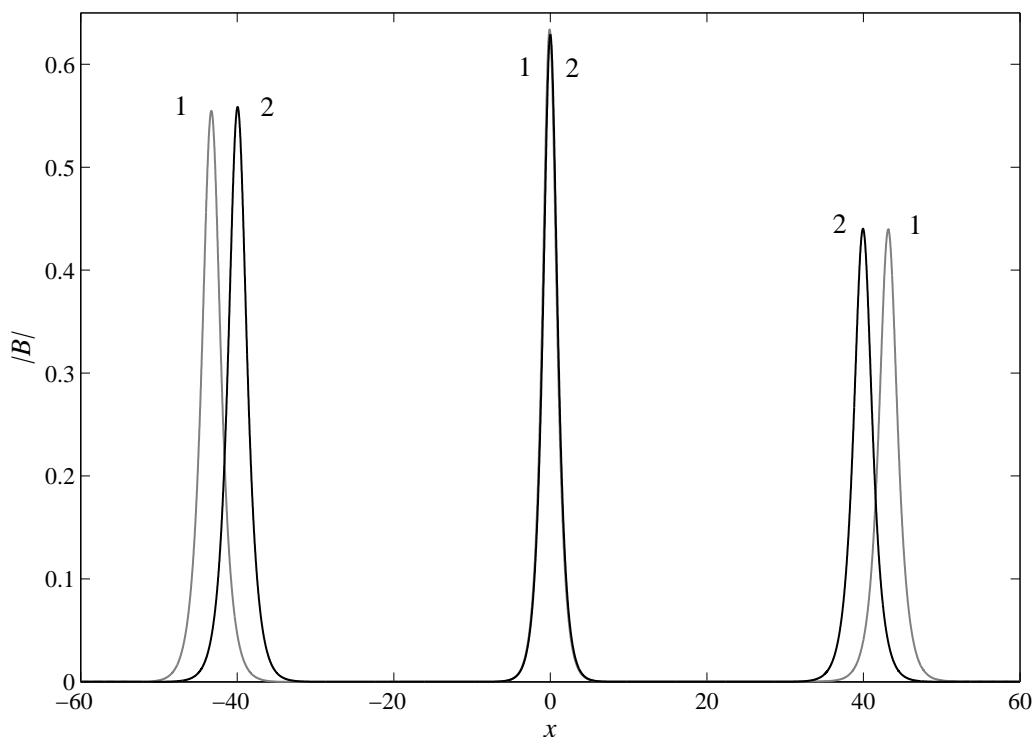


FIGURE 14. cDZ-Dysthe equation: Initial (1) shape and (2) after collision of the two traveling waves and a ground state ($\varepsilon = 0.10$).

- [36] V. E. Zakharov. Stability of periodic waves of finite amplitude on the surface of a deep fluid. *J. Appl. Mech. Tech. Phys.*, 9:190–194, 1968. [1](#), [2](#)
- [37] V. E. Zakharov. Statistical theory of gravity and capillary waves on the surface of a finite-depth fluid. *Eur. J. Mech. B/Fluids*, 18(3):327–344, 1999. [2](#)
- [38] V. E. Zakharov and A. I. Dyachenko. About shape of giant breather. *Eur. J. Mech. B/Fluids*, 29(2):127–131, 2010. [4](#)
- [39] V. E. Zakharov, P. Guyenne, A. N. Pushkarev, and F. Dias. Wave turbulence in one-dimensional models. *Physica D*, 153:573–619, 2001. [6](#)
- [40] V. E. Zakharov and A. B. Shabat. Exact Theory of Two-dimensional Self-focusing and One-dimensional Self-modulation of Waves in Nonlinear Media. *Soviet Physics-JETP*, 34:62–69, 1972. [2](#)

SCHOOL OF CIVIL AND ENVIRONMENTAL ENGINEERING & SCHOOL OF ELECTRICAL AND COMPUTER ENGINEERING, GEORGIA INSTITUTE OF TECHNOLOGY, ATLANTA, USA

E-mail address: fedele@gatech.edu

URL: <http://savannah.gatech.edu/people/ffedele/Research/>

LAMA, UMR 5127 CNRS, UNIVERSITÉ DE SAVOIE, CAMPUS SCIENTIFIQUE, 73376 LE BOURGET-DU-LAC CEDEX, FRANCE

E-mail address: Denys.Dutykh@univ-savoie.fr

URL: <http://www.lama.univ-savoie.fr/~dutykh/>